

## Influence of Electron Beam Irradiation on the Mechanical and Thermal Properties of Polypropylene/Polyamide6 Blends

Shigeya Nakamura,<sup>1,2</sup> Katsuhisa Tokumitsu,<sup>1</sup> Tohru Yamaguchi<sup>3</sup>

<sup>1</sup>Department of Materials and Science School of Engineering, The University of Shiga Prefecture, 2500 Hassaka-cho, Hikone, Shiga 522-8533, Japan

<sup>2</sup>Hitachi Chemical Co., Ltd., 1150 Goshomiya, Chikusei, Ibaraki 308-8524, Japan

<sup>3</sup>Japan Electron Beam Irradiation Service Co., Ltd., 4-16 Midorigahara, Tsukuba, Ibaraki 300-2646, Japan

Correspondence to: K. Tokumitsu (E-mail: ktokumit@mat.usp.ac.jp)

**ABSTRACT:** This article investigates the effects of electron beam irradiation on the mechanical and thermal properties of polypropylene/polyamide6 blends (45/55) with talc 20% (w/w) as filler, SEBS-g-MAH 5% (w/w) as compatibilizer, and 10 phr triallyl isocyanurate (TAIC). TAIC is a polyfunctional monomer and acts as a crosslinking agent. Although the tensile and flexural moduli and strengths of the PP/PA6 blends with talc, SEBS-g-MAH, and TAIC were increased by the application of electron beam irradiation, the impact strength was decreased. Differential scanning calorimetry measurements showed that the melting temperatures and the degree of crystallinity decreased for all PP/PA6 blends as the electron beam irradiation dose increased, because of the number of structural defects in each crystalline phase. From dynamic mechanical analyzer results, a storage modulus curve in the plateau region was observed only in the PP/PA6 blends with talc, SEBS-g-MAH, and TAIC. The modulus increased with increasing electron beam irradiation dose, indicating that the three-dimensional network developed gradually in the more amorphous PA6. Consequently, the most significant improvement to heat distortion under high load (1.8 MPa) was observed at 200 kGy. © 2013 Wiley Periodicals, Inc. *J. Appl. Polym. Sci.* 130: 4318–4326, 2013

**KEYWORDS:** polyolefins; polyamides; blends; irradiation; mechanical properties

Received 9 March 2013; accepted 19 May 2013; Published online 17 July 2013

**DOI:** 10.1002/app.39584

### INTRODUCTION

Polypropylene (PP) is widely used in automobile parts and consumer goods. It is attractive because of its cost-efficient performance, high processability, and high resistance to water and chemicals. However, increasing complexity of consumer products means that it is difficult to satisfy all material requirements using only PP; therefore, the characteristics of PP must be modified. To improve the physical and mechanical properties of PP, it can be blended with inorganic fillers such as silica,<sup>1,2</sup> CaCO<sub>3</sub>,<sup>3,4</sup> talc,<sup>5–8</sup> clay,<sup>9</sup> and silica rock.<sup>10,11</sup> It has been reported that the effectiveness of the inorganic filler in a PP composite strongly depends on the shape, size, and aspect ratio of the filler, as well as the interfacial adhesive strength and quality of the dispersion.<sup>12–14</sup> Talc is known to be one of the most effective means for improving the hardness and heat resistance of PP composite materials.

There have been many studies reporting the improvement of the mechanical properties of polymer blends and alloys; this has been achieved by adding polymer materials such as polyethylene

terephthalate,<sup>15</sup> polycarbonate,<sup>16</sup> polyethylene (PE),<sup>17</sup> ethylene-propylene rubber,<sup>18</sup> and polyamide (PA).<sup>19,20</sup> Notable studies have done by Ide et al.<sup>21</sup> and Duvall et al.<sup>19</sup> looking at the morphological and mechanical properties of a PP/PA blend with maleic anhydride-grafted polypropylene (PP-g-MAH) as a compatibilizer.

Polymer crosslinking caused by  $\gamma$  radiation and electron beam irradiation improves physical and chemical properties such as the hardness, Young's modulus, thermal resistance, and solubility. Electron irradiation crosslinking, in particular, is widely used in industrial applications for products such as insulation cables, radial tires, heat-shrinking tubes and sheets, and foams.<sup>22</sup> There have been many reports on the  $\gamma$  irradiation and electron beam irradiation of PP.<sup>23,24</sup> Yoshii et al. investigated the irradiation damage on PP by electron beam and  $\gamma$  irradiation, and quantified the oxidation and mechanical properties. It was clear that electron beam irradiation was less damaging on PP than  $\gamma$  irradiation.<sup>25–27</sup> In general, molecular scission dominates the formation of a crosslinked structure in irradiated PP.

Crosslinking in PP is achieved via the addition of a crosslinking agent<sup>24–30</sup> and an elastomer.<sup>31,33</sup> Sawasaki and Nojiri<sup>29</sup> investigated a gel fraction to confirm that crosslinking by varying the irradiation dose and using a polyfunctional monomer (PFM) with various functional numbers as a crosslinking agent. They found that a PFM with three or more acryloyloxy groups was most suitable for achieving crosslinking in PP. An appropriate amount of antioxidant is important to prevent the degradation reaction of PP, which was caused by the electron beam irradiation. It was also important that a minimum irradiation dose was used. They found that the crosslinked PP showed a high Young's modulus at high temperatures and high impact strength, and existed in a rubber-like state at the melting point. Han et al.<sup>30</sup> reported that homo-PP including triallyl cyanurate showed higher radiation stability than trimethylpropane triacrylate (TMPTA), and that random terpolymer PP including TMPTA had good radiation stability. It was suggested that PP crosslinking mainly occurs at the boundary surface between the crystalline and amorphous regions.

Steller et al. found that PP blended with styrene-ethylene/butylene-styrene (SEBS) was more resistant to radiation than PP with styrene-butadiene-styrene (SBS). Irradiation of PP/SBS blends led to structural changes in the crystalline and amorphous PP phase, and in the elastic SBS phase.<sup>31</sup>

There have been many studies investigating electron beam irradiation of PA.<sup>3,4,33,34</sup> Aytac et al. studied the effects of  $\gamma$  irradiation and electron beam irradiation on the mechanical properties of PA6 and PA66 fabrics.<sup>33</sup> They found that  $\gamma$  irradiation caused a larger decline in the mechanical properties in both materials than caused by electron beam irradiation. Pramanik et al. confirmed that the irradiation of PA66 led to an improved modulus and decreased the speed of thermolysis.<sup>34</sup> It was proposed that this result was caused by the formation of a three-dimensional (3D) network. The crosslinking and molecular scission caused by electron beam irradiation for PP, PA, and blended materials such as PP/PE,<sup>35</sup> PE/ethylene vinylacetate copolymer,<sup>36</sup> and poly(lactic acid)/poly(butylene terephthalate-co-adipate)<sup>37</sup> has been studied. However, PP/PA6 blends have not been investigated as thoroughly.

The main aim of this study is to improve the mechanical and thermal properties of PP/PA6 blends with talc in the base blend, using electron beam irradiation. We report the effects on mechanical and thermal properties of adding SEBS-g-MAH (which acted as a compatibilizer) and triallyl isocyanurate (TAIC; which acted as a crosslinking agent) to the base blend. The formation of the crosslinked structure was confirmed using dynamic viscoelastic measurements.

## EXPERIMENTAL

### Materials

The materials used in this study were (i) PP, W101 supplied by Sumitomo Chemical Co., Ltd., Japan, (ii) PA6, T803 supplied by Toyobo, Japan, (iii) SEBS-g-MAH (acting as a compatibilizer for the PP and PA6), supplied by Kraton Polymer, Japan, (iv) talc (acting as a filler), MS-P supplied by Japan Talc, Japan (the diameter of the talc was 12.4  $\mu\text{m}$ ), and (v) TAIC (acting as a

**Table I.** Characteristics of Neat PP and PA6

Samples	Density (g/cm <sup>3</sup> )	MFR (g/10 min)	Young's modulus (MPa)	Yield stress (MPa)
PP	0.9	3	1,585	33
PA6	1.14	55	1,729	51.3

crosslinking agent), Japan Chemical, Japan. Table I shows the characteristics of the neat PP and PA6.

### Preparation of the Blends

The melt compounding of the PP/PA6 blends was conducted in two steps. In the first step, PP/PA = 45/55, with/without 5% (w/w) SEBS-g-MAH, was blended using a 25-mm diameter co-rotating twin-screw extruder (KTW-15TW-45HG-NH-700-SG, Technovel) with a length to diameter ratio ( $L/D$ ) of 45. Two raw material supply machines were provided for this extruder. The cylinder temperature was 240°C. A bag of premixed PP, PA6 and the SEBS-g-MAH was fed through the main feeder to the extruder. The screw was rotated at 250 rpm. In the second step, the PP/PA6 blend with/without of SEBS-g-MAH added to talc (20%, w/w) and the PP/PA6 blend with SEBS-g-MAH added to talc (20%, w/w) and TAIC (10 phr) were compounded using a 40-mm diameter co-rotating twin-screw extruder (HK25D, Parker) with an  $L/D$  ratio of 40. Two raw material supply machines were also provided for this extruder. The cylinder temperature was 240°C. PP/PA6 blends with/without SEBS-g-MAH were fed from the main feeder, while talc and TAIC were fed through the side feeder to the extruder. The screw was rotated at 250 rpm. Prior to processing, the PA6 and PP/PA6 blends with/without SEBS-g-MAH were vacuum dried for at least 5 h at 80°C.

### Preparation of the Films

Film samples of several PP/PA6 blends with and or without talc, SEBS-g-MAH, and TAIC were prepared using injection molding. Injection molding was carried out at 240°C. Prior to injection molding, the blended samples were dried at 80°C for 3 h.

### Electron Beam Irradiation of the Films

The PP/PA6 blend films with talc, SEBS-g-MAH, and TAIC were subjected to 2 MeV pulsed electron beam irradiation (RDI Dynamitron accelerator), in air and at ambient temperature. This was tested at the Japan Electron Beam Irradiation Service, Japan. The irradiation doses were 50, 100, and 200 kGy.

### Tensile Tests

The tensile tests were carried out according to ISO527 using a dumbbell-shaped specimen on an AG-1 instrument (Shimadzu Seisakusho) at ambient temperature. The cross-head speed was 50 mm/min, and the dimensions of the specimens were 115 mm in initial length, 10 mm in width, and 4 mm in thickness.

### Flexural Tests

The flexural tests were carried out according to ISO178, using an EZ-test instrument (Shimadzu Seisakusho) at ambient

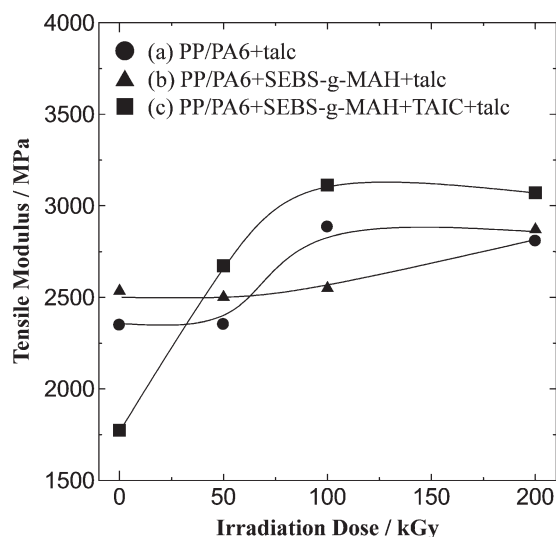


**Figure 1.** Variation of the tensile modulus with irradiation dose: (a) PP/PA6+talc, (b) PP/PA6+SEBS-g-MAH+talc, and (c) PP/PA6+SEBS-g-MAH+TAIC+talc.

temperature. The cross-head speed was 2 mm/min. The maximum load was obtained, and the flexural strength ( $\gamma$ ) was calculated using the following formula:

$$\sigma = 3FL / (2BH^2) \quad (1)$$

where  $F$  is the maximum load,  $L$  is the distance between the supports (64 mm),  $B$  is the width of the specimen (10 mm), and  $H$  is the height (4 mm). The modulus of elasticity was determined using the following expression:

$$E = FL^3 / 4BH^3 d \quad (2)$$

where  $d$  is the deflection value when the load was applied.

### Charpy Impact Tests

Charpy impact tests were carried out according to ISO179, using an impact tester (Yasudaseiki Seisakusho, No.141-IS) at ambient temperature. The energy of the impact hammer was 2 J, and a single-notched specimen (Type A-4E) was used.

### Heat Distortion Test Analysis

Heat distortion tests were carried out according to ISO75, using a heat distortion tester (Toyouseiki Seisakusho, S3-MH). The temperature was raised from 30°C at a rate of 120°C/min. The distance between the supports was 64 mm. The loads used were 0.45 and 1.8 MPa. The heat distortion temperature was measured at 0.34 mm of bending.

### DSC Analysis

Thermal analysis was carried out under a nitrogen atmosphere, using a differential scanning calorimeter (Shimadzu Seisakusho, DSC-60-A). The temperature was raised from 40 to 250°C at a rate of 10°C/min. The degrees of crystallinity in the PP and PA6 phases of the PP/PA6 blend ( $X_C^{PP}$  and  $X_C^{PA6}$ ) were determined, taking into account the weight ratio of the PP phase and the PA6 phase ( $M_{PP}$  and  $M_{PA6}$ ):

$$X_C^{PP}(\%) = \frac{\Delta H_{PP}^{Sample}}{\Delta H_{PP}^{Cry} \times M_{PP}} \times 100 \quad (3)$$

$$X_C^{PA6}(\%) = \frac{\Delta H_{PA6}^{Sample}}{\Delta H_{PA6}^{Cry} \times M_{PA6}} \times 100 \quad (4)$$

where  $\Delta H_{PP}^{Sample}$  and  $\Delta H_{PA6}^{Sample}$  represent the heat of fusion of the PP phase and PA6 phase in the sample. The heat of fusion for the 100% crystallinity of PP ( $\Delta H_{PP}^{Cry}$ ) and PA6 ( $\Delta H_{PA6}^{Cry}$ ) was 209.1 and 184.1 J/g, respectively.

### DMA Analysis

Dynamic mechanical analysis (DMA) was carried out using a dynamic viscoelastometer (Rheogel E-4000; UBM, Japan) in tensile mode, with an initial chuck distance of 20 mm. The applied frequency was 8 Hz, and a heating rate of 3°C/min was applied over the temperature range from -150 to 250°C. The size of the test specimen was 1.0 mm in thickness, 3 mm in width, and 30 mm in length.

### SEM Observation

Scanning electron microscope (SEM) observation was carried out by VE9800 (Keyence, Japan). Morphological change in the sample surfaces after impact tests was estimated.

## RESULTS AND DISCUSSION

Figure 1 shows the irradiation dose effects on the tensile modulus of the PP/PA6 blend with talc, SEBS-g-MAH (acting as a compatibilizer), and TAIC (acting as a crosslinking agent). The tensile modulus of the PP/PA6 blends with talc and with/without SEBS-g-MAH increased by approximately 120% at 200 kGy compared with the value measured before irradiation. The tensile modulus of the PP/PA6 blend with talc, SEBS-g-MAH, and TAIC decreased by 25% compared with the value before irradiation, but showed the highest value at 100 kGy. This result indicated that the stiffness of the PP/PA6 blend with talc, SEBS-g-MAH, and TAIC was increased by the electron beam irradiation.

Figure 2 shows the irradiation dose effects on the tensile strength of the PP/PA6 blend with talc, SEBS-g-MAH, and TAIC. The changes to the tensile strength caused by the irradiation dose were similar to the trends observed for the tensile modulus. It was found that the tensile strength of the PP/PA6 blend with talc was 39 MPa before irradiation. The strength at 200 kGy increased to 44 MPa. When SEBS-g-MAH was added to the PP/PA6 blend with talc, the tensile strength increased to 47 MPa before irradiation. This result indicated that the interfacial adhesion between PP and PA6 was improved by the use of SEBS-g-MAH as a compatibilizer.<sup>20</sup> The strength of the PP/PA6 blend with talc and SEBS-g-MAH was 53 MPa at 200 kGy. The increases in the electron beam irradiation were the same as those used for the sample without SEBS-g-MAH. However, when SEBS-g-MAH and TAIC were added to the PP/PA6 blend with talc, the tensile strength increased significantly, to 64 MPa.

Figures 3 and 4 show the effects of changes in the irradiation dose on the flexural modulus of the PP/PA6 blend with talc, SEBS-g-MAH, and TAIC. The flexural modulus of the PP/PA6 blend with/without SEBS-g-MAH slightly increased as the irradiation

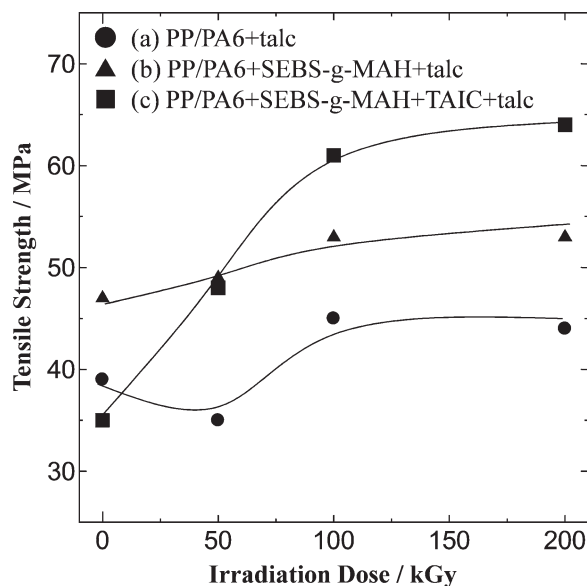


**Figure 2.** Variation of the tensile strength with irradiation dose: (a) PP/PA6+talc, (b) PP/PA6+SEBS-g-MAH+talc, and (c) PP/PA6+SEBS-g-MAH+TAIC+talc.

dose increased. In particular, adding SEBS-g-MAH and TAIC into the PP/PA6 blend with talc significantly increased the flexural modulus at 100 kGy by up to 150% compared with the PP/PA6 blend with talc. The changes in flexural strength with the irradiation dose were similar to the behavior observed for the flexural modulus. The flexural strength of the PP/PA6 blend with talc, SEBS-g-MAH, and TAIC increased at 100 kGy by 225% compared with the PP/PA6 blend with talc before irradiated. Therefore, it was deduced that the improvements in the flexural properties that resulted from the addition of SEBS-g-MAH and TAIC to the PP/PA6 blend were due to the crosslinked structure formed in PA6 during the electron beam irradiation. These results indicate that the most suitable irradiation dose, which resulted in the

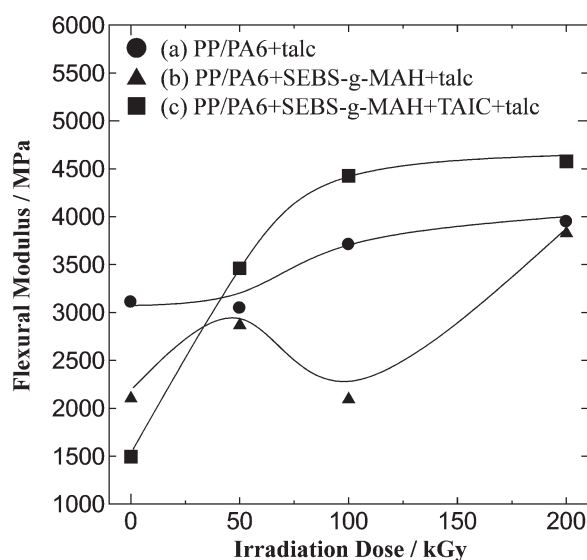


**Figure 3.** Variation of the flexural modulus with irradiation dose: (a) PP/PA6+talc, (b) PP/PA6+SEBS-g-MAH+talc, and (c) PP/PA6+SEBS-g-MAH+TAIC+talc.

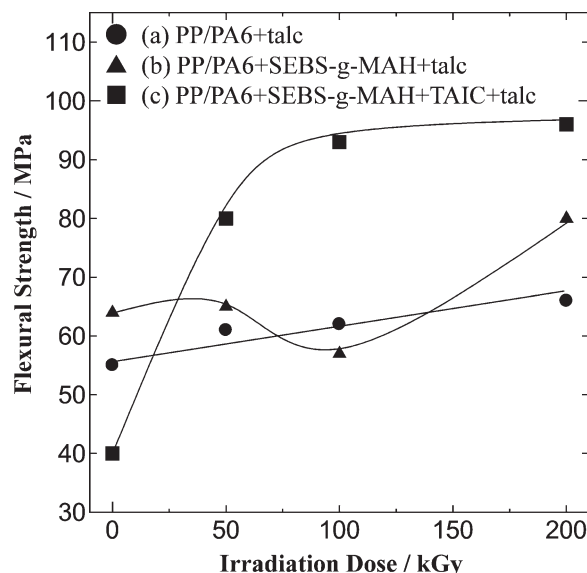


**Figure 4.** Variation of the flexural strength with irradiation dose: (a) PP/PA6+talc, (b) PP/PA6+SEBS-g-MAH+talc, and (c) PP/PA6+SEBS-g-MAH+TAIC+talc.

most improved mechanical properties, was 100 kGy. The degradation of the molecular chains and the creation of the crosslinked structures proceeded simultaneously under the electron beam irradiation. The dominant process was dependent on the polymer chemical structure. It has been previously reported that the degradation process dominates for PP, resulting in a decreased modulus and yield stress. In this study, no change to the mechanical properties of the PP/PA6 blend with talc and SEBS-g-MAH under the electron beam irradiation was detected. Considering that the ultimate tensile stress and the 10% modulus of a PA66 film irradiated at 200 kGy was significantly better than the performance of the nonirradiated film reported by Sengupta et al.,<sup>3</sup> it was deduced that the crosslinked structures formed in PA6 by electron beam irradiation play an important role in enhancing the mechanical properties of PP/PA6 blends. Moreover, the SEBS-g-MAH used in this study acted not only as a compatibilizer for PP and PA6, but also as a crosslinking agent between the PP and PA6 phases because of the irradiation-promoted crosslinking structures of elastomers. These crosslinking structures, such as EPDM,<sup>38</sup> SBS,<sup>39</sup> and SEBS,<sup>35</sup> have been previously reported.

Table II shows the Charpy impact strength of the PP/PA6 blends with different irradiation dose. Although the impact strength

**Table II.** Charpy Impact Strength with Irradiation Dose: (a) PP/PA6+talc, (b) PP/PA6+SEBS-g-MAH+talc, and (c) PP/PA6+SEBS-g-MAH+TAIC+talc

Irradiation dose (kGy)	(a) PP/PA6 with talc	(b) PP/PA/SEBS-g-MAH with talc	(c) PP/PA/SEBS-g-MAH with TAIC and talc
0	2.7	4.6	5.7
50	2.8	4.0	4.1
100	2.5	3.5	3.1
200	2.3	3.3	2.8

**Table III.** HDT with Irradiation Dose: (a) PP/PA6+talc, (b) PP/PA6+SEBS-g-MAH+talc, and (c) PP/PA6+SEBS-g-MAH+TAIC+talc

Irradiation dose (kGy)	(a) PP/PA6+talc		(b) PP/PA6+SEBS-g-MAH+talc		(c) PP/PA6+SEBS-g-MAH+TAIC+talc	
	0.45 MPa	1.8 MPa	0.45 MPa	1.8 MPa	0.45 MPa	1.8 MPa
0	155	63	142	56	96	55
50	140	68	124	58	139	64
100	134	71	141	60	141	73
200	145	73	144	60	150	84

continuously decreased with increasing irradiation dose for all of the blends, no significant differences were observed between the impact strengths of the blends irradiated with different doses.

Table III shows the heat distortion temperatures at different irradiation doses for the PP/PA6 blend with talc, SEBS-g-MAH, and TAIC. Under a low load (0.45 MPa), the heat distortion temperature at 200 kGy was approximately 145°C for all of the blends. No significant effects resulted from either the addition of SEBS-g-MAH and TAIC to the PP/PA6 blend with talc, or the application of electron beam irradiation, owing to effects of the reinforcement using 20% (w/w) talc as a filler. However, the reinforcing effects of the talc were not apparent under a high load (1.8 MPa). Figure 5 shows the variation of the heat distortion temperature as a function of the irradiation dose, under a high load (1.8 MPa). Before irradiation, the PP/PA6 blend with talc had a heat distortion temperature of 63°C, and SEBS-g-MAH (which was made up of rubber constituents) made the stiffness lower, resulting in a decrease in the temperature to 55°C. The level of improvement after the application of electron beam irradiation was almost the same for the base blends with/without SEBS-g-MAH. This result also supported the result

mentioned above that crosslinked structures formed in the PA6 phase. However, the PP/PA6 blend with talc, SEBS-g-MAH, and TAIC showed significant improvement in the heat distortion temperature. As a result, a 3D network developed, owing to the crosslinked structure formed in the PA6 molecular chain by electron beam irradiation.

The DSC method made it possible to determine the melting point and heat of fusion of each phase—dispersed phase and matrix one—in the blends, individually. Table IV shows the melting temperature, the heat of fusion, and the degree of crystallinity results for the PP and PA6 phases in the PP/PA6 blends. In all of the blends, the melting temperature of each phase decreased with increasing irradiation dose. For the PP/PA6 blend with talc, SEBS-g-MAH, and TAIC irradiated with 200 kGy, the melting temperature in the PP and PA6 phases shifted drastically from 164.3 to 149.5°C, and from 221.4 to 206.4°C, respectively. This phenomenon was due to the greater change in fusion entropy as a result of molecular degradation by the electron beam irradiation. It was also deduced that the crosslinked structures of PP and/or PA6 act as structural defects in each of the molecular chains. The defect in the molecular chain was moved from the crystalline region to the noncrystalline region. The more structural defects that are present in the noncrystalline region, the harder the thick lamella crystal forms because of the shortness of the effective molecular chain length that can crystallize. The variations in the degree of crystallinity with irradiation dose are shown in Figure 6 for each phase. The electron beam irradiation led to an increase in the degree of crystallinity for only the PP phase with radiation dose in the PP/PA6 blend with talc. It is likely that the increase in the degree of crystallinity for the PP phase resulted from the fact that degraded PP molecular chains act as crystal nucleation agents. In the case of the PP/PA6 blend with talc and SEBS-g-MAH, the degree of crystallinity decreased with irradiation dose for both phases. This phenomenon was attributed to an increased number of structural defects in each crystalline phase, caused by radiation, and/or to more intense interactions between the PP matrix and the PA6 matrix with SEBS-g-MAH, which is also a result of the electron irradiation.<sup>31</sup> In the case of the PP/PA6 blend with talc, SEBS-g-MAH, and TAIC, the degree of crystallinity for the PP phase slightly decreased at 200 kGy to approximately 27%. In contrast, the degree of crystallinity in the PA6 phase rapidly decreased when the irradiation was increased to 50 kGy, reaching its ultimate value of approximately 12%. These findings are the result the 3D network that was developed in the PA6 molecular chains under the electron beam irradiation, causing an

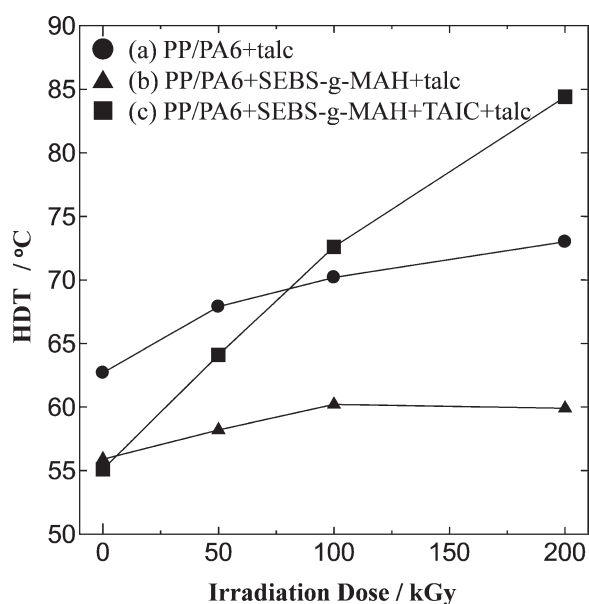


**Figure 5.** Variation of the HDT with irradiation dose: (a) PP/PA6+talc, (b) PP/PA6+SEBS-g-MAH+talc, and (c) PP/PA6+SEBS-g-MAH+TAIC+talc.

**Table IV.** Melting Temperature, Heat of Fusion, and Degree of Crystallinity of PP and PA6 in PP/PA6 Blends with Different Irradiation Dose from 0 to 200 kGy

Materials	Irradiation dose (kGy)	Melting temperature °C		Heat of fusion (J/g)		Degree of crystallinity (%)	
		PP phase	PA6 phase	PP phase	PA6 phase	PP phase	PA6 phase
(a) PP/PA6+talc	0	168.5	223.0	23.6	22.9	31.3	27.3
	50	163.1	221.8	21.6	20.1	28.7	23.9
	100	159.9	221.3	22.9	21.9	30.4	26.1
	200	157.7	221.4	25.0	20.2	33.2	24.1
(b) PP/PA6+SEBS-g-MAH+talc	0	168.5	223.0	23.6	22.9	31.3	27.3
	50	163.9	221.9	24.8	22.3	32.9	26.5
	100	162.4	221.3	19.5	18.6	25.9	22.1
	200	160.7	221.7	14.2	10.4	18.8	12.4
(c) PP/PA6+SEBS-g-MAH+TAIC+talc	0	164.3	221.4	22.0	20.7	29.2	24.7
	50	157.4	211.8	19.8	13.4	26.3	15.9
	100	151.1	200.4	20.2	12.6	26.9	15.0
	200	149.5	206.4	20.2	10.4	26.8	12.4

improvement in the tensile strength and the flexural strength. It is likely that the improved mechanical properties also result from the crystal domain sizes being enlarged by the electron beam irradiation, where the crystal domains acted to concentrate the stress.<sup>24</sup>

DMA measurements were used to estimate the molecular motion for the PP/PA6 blend films as a function of temperature; the variations in the storage modulus ( $E'$ ) and  $\tan \delta$  are shown in Figure 7. For PP, the  $\gamma$  relaxation at approximately  $-125^\circ\text{C}$  and the  $\beta$  relaxation at approximately  $-10^\circ\text{C}$  were attributed to the side chain relaxation and local main chain relaxation in the amorphous region, respectively. For PA6, on the other hand, the  $\beta$  relaxation at approximately  $-55^\circ\text{C}$  and the  $\alpha$  relaxation at approximately  $60^\circ\text{C}$  corresponded to the

main chain relaxation and local main chain relaxation in the amorphous region, respectively. For the PP/PA6 blended with talc, the intensity of  $E'$  decreased with irradiation dose. The  $\gamma$  relaxation in PP for the PP/PA6 blend with talc at approximately  $-120^\circ\text{C}$  shifted to lower temperatures, and the intensity of the peak increased with increasing irradiation dose. The peak temperature and  $\beta$  relaxation of PA6 shifted to lower temperatures, and the intensity of its peak increased [Figure 7(a)]. This result indicated that the degradation of PP and PA6 increased under electron beam irradiation. In the case of the PP/PA6 blend with talc and SEBS-g-MAH, the decrease in  $E'$  with room temperature was not observed. This result showed that the interfacial adhesion between PP and PA6 increased after the addition of SEBS-g-MAH as a compatibilizer. The changes in  $\tan \delta$  that resulted from changes in the irradiation dose were

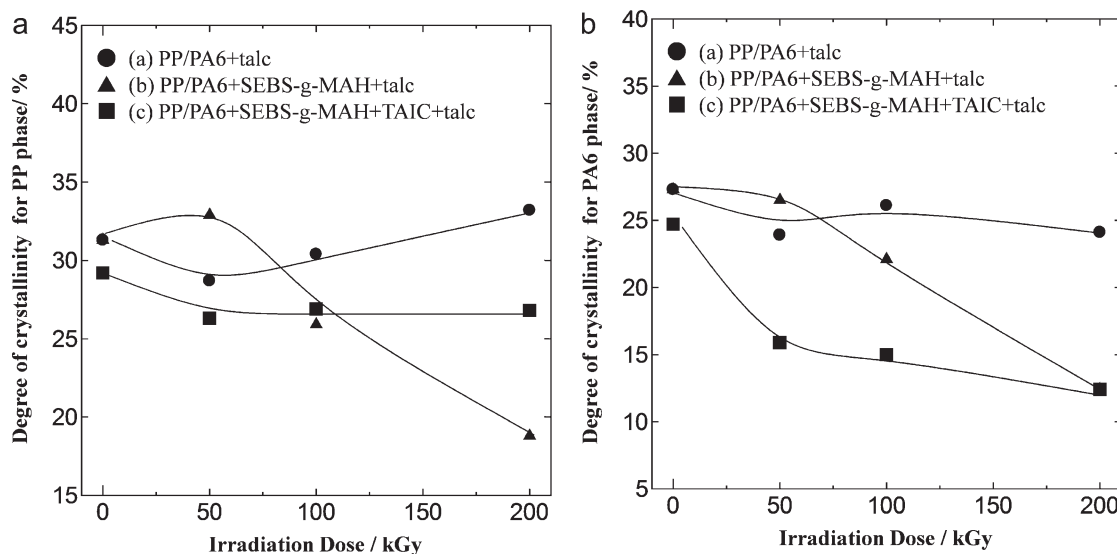


**Figure 6.** Variation of the degree of crystallinity with irradiation dose: (a) PP/PA6+talc, (b) PP/PA6+SEBS-g-MAH+talc, and (c) PP/PA6+SEBS-g-MAH+TAIC+talc.

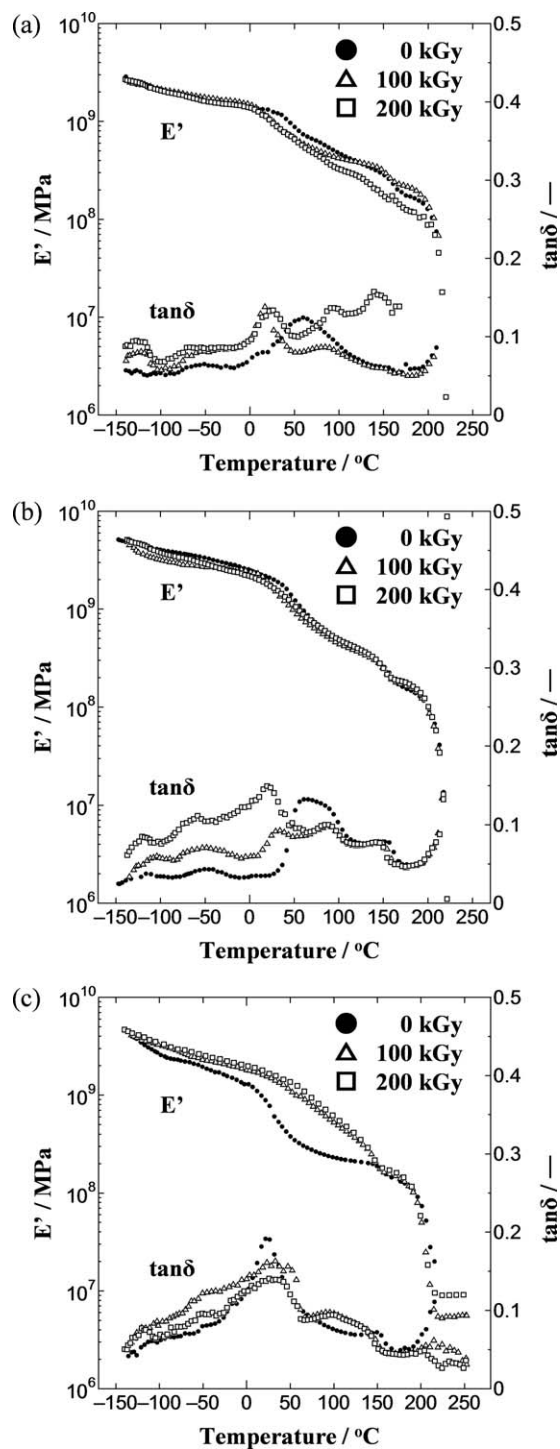


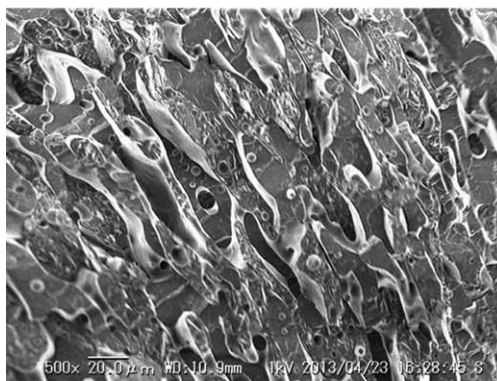
**Figure 7.** Storage modulus ( $E'$ ) and  $\tan \delta$  curves with/without EB irradiation: (a) PP/PA6+talc, (b) PP/PA6+SEBS-g-MAH+talc, and (c) PP/PA6+SEBS-g-MAH+TAIC+talc.

similar to those observed for the PP/PA6 blend with talc. These results indicated that the degradation of the PP/PA6 blend with/without SEBS-g-MAH dominated over the crosslinking [Figure 7(b)]. Interestingly, in the case of the base blend with SEBS-g-MAH and TAIC, it was observed that the  $E'$  of the irradiated films showed a plateau region from approximately

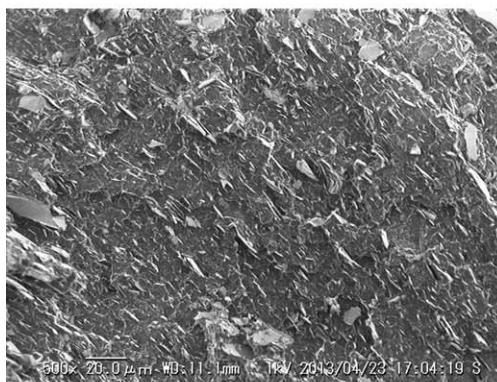
200°C; this represented the melting temperature of PA6, and the modulus increased with increasing irradiation dose. In addition, it was observed from  $\tan \delta$  that the  $\beta$  relaxation of PA6 shifted to higher temperatures and the modulus of the peak decreased with increasing irradiation dose. This result confirmed that the crosslinked structure of PA6 was formed by the electron beam irradiation, and that the crosslinking increased with increasing irradiation dose [Figure 7(c)].

Figure 8 shows the morphology of the different PP/PA6 blends before irradiation. In the case of the PP/PA6 blend with talc,

**(a) PP/PA6+Talc**



**(b) PP/PA6+SEBS-g-MAH+Talc**



**(c) PP/PA6+SEBS-g-MAH+TAIC+Talc**

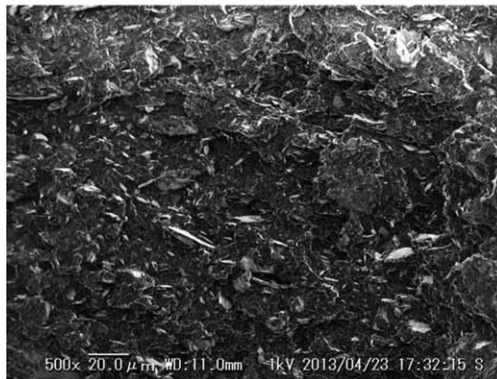
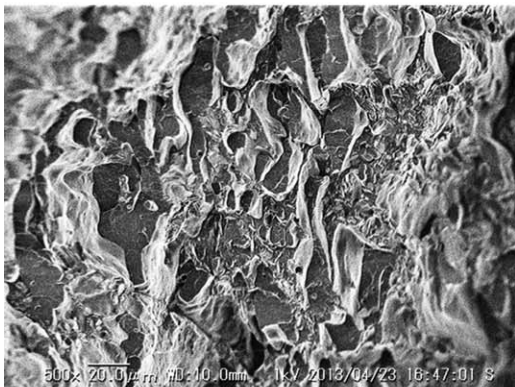
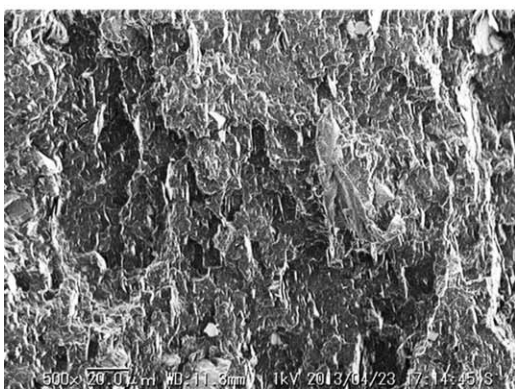


**Figure 8.** SEM micrographs of PP/PA6 blends before irradiation: (a) PP/PA6+Talc, (b) PP/PA6+SEBS-g-MAH+Talc, and (c) PP/PA6+SEBS-g-MAH+TAIC+Talc.

(a) PP/PA6+Talc



(b) PP/PA6+SEBS-g-MAH+Talc



(c) PP/PA6+SEBS-g-MAH+TAIC+Talc

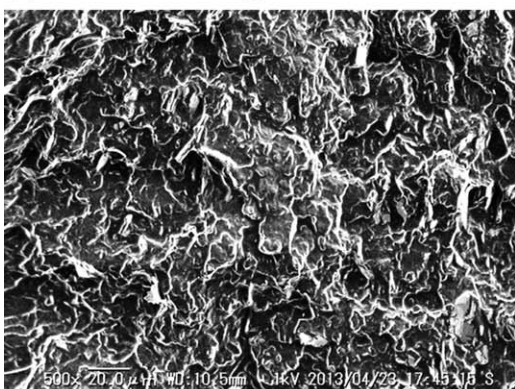


**Figure 9.** SEM micrographs of PP/PA6 blends after irradiation with 200 kGy: (a) PP/PA6+Talc, (b) PP/PA6+SEBS-g-MAH+Talc, and (c) PP/PA6+SEBS-g-MAH+TAIC+Talc.

the PP phase forms the matrix and the PA6 phase is segregated into a spherical domain [Figure 8(a)]. No morphological evidence of good adhesion at the interphase between PP and PA6 can be seen. In addition to SEBS-g-MAH as a compatibilizer, it is difficult to find continuous and dispersed phases [Figure 8(b)]. No morphological change was observed by adding the TAIC as a crosslinking agent [Figure 8(c)].

Figure 9 shows the effects on morphology of different PP/PA6 blends after irradiation with 200 kGy. In the case of the PP/PA6

blend with talc, morphological change to the rough surface was observed [Fig. 9(a)]. This tendency was observed for the other PP/PA6 blends. It was deduced that the morphological change resulted from the degradation of PP and PA6 and/or the crosslinking in the PA6 domains caused by electron beam irradiation.

## CONCLUSIONS

In this study, the effects of electron beam irradiation on the mechanical and thermal properties and the molecular kinetics of PP/PA6 blends with added talc, SEBS-g-MAH (which acted as a compatibilizer), and TAIC (which acted as a crosslinking agent) were investigated. The results are concluded as follows:

1. When SEBS-g-MAH and TAIC were added to the PP/PA6 blend with talc, the mechanical and thermal properties were improved by electron beam irradiation. The tensile and flexural strength increased with increasing irradiation dose. The optimum radiation dose level was 200 kGy, which showed the most significant improvement in the heat distortion temperature under a high load (1.8 MPa).
2. It was confirmed from DSC analysis that for PP/PA6 blended with talc, SEBS-g-MAH, and TAIC, increases in the irradiation dose leads to decreased melting temperature and degree of crystallinity of the PP and PA6 phases. This phenomenon was attributed to an increase in the number of structural defects in each crystalline phase, which was caused by the radiation and/or more intense interactions between the PP matrix and the PA6 matrix with SEBS-g-MAH.
3. DMA results confirmed that the crosslinked structure of PA6 formed as a result of the electron beam irradiation. The intensity of the  $\beta$  relaxation of PA6 showed some correlation with the irradiation dose, which decreased the  $\beta$  relaxation intensity in PA6, and resulted in an increase in the temperature. The storage modulus curve in the plateau region was observed only for the PP/PA6 blends with talc, SEBS-g-MAH, and TAIC; the modulus increased with increasing electron beam irradiation dose, indicating that the 3D network developed gradually in the more amorphous PA6. It was found that the most significant improvement in heat distortion under a high load (1.8 MPa) was observed at 200 kGy.

## REFERENCES

1. Petrovicova, R.; Knight, R.; Schadler, L. S.; Twadowshi, T. E. *J. Appl. Polym. Sci.* **2000**, *78*, 2272.
2. Petrovics, Z. S.; Javni, I.; Waddon, A.; Banhegi, G. *J. Appl. Polym. Sci.* **2000**, *76*, 133.
3. Sengupta, R.; Tikku, V. T.; Somani, A.; Chaki, T. K.; Bhowmick, A. K. *Radiat. Phys. Chem.* **2005**, *72*, 751.
4. Van Dyke, J. D.; Gnatowski, M.; Koutsandres, A.; Burczyk, A.; Duncan, S. *J. Appl. Polym. Sci.*, **2003**, *89*, 980.
5. Ferrage, E.; Martin, F.; Boudet, A.; Petit, S.; Fourty, G.; Jouffret, F.; Micoud, P.; De Parseval, P.; Salvi, S.; Bourgerette, C.; Ferret, J.; Saint-Gerard, Y.; Buratto, S.; Fortune, P. *J. Mater. Sci.* **2002**, *37*, 1561.



6. Zihlif, A. M.; Ragosta, G. *Mater. Lett.* **1991**, *11*, 368.
7. Zhou, Y.; K. Mallick, P. *Polym. Eng. Sci.* **2002**, *42*, 2449.
8. Zhou, Y.; Rangari, V.; Mahfuz, H. V.; Jeelani, S.; Mallick, P. K. *Mater. Sci. Eng. A* **2005**, *402*, 109.
9. Hambir, S.; Bulakh, N.; Jog, J. P. *Polym. Eng. Sci.*, **2002**, *42*, 1800.
10. Hadal, R. S.; Dasari, A.; Rohrmann, J.; Misra, R. D. K. *Mater. Sci. Eng. A* **2004**, *372*, 296.
11. Hadal, R. S.; Misra, R. D. K. *Mater. Sci. Eng. A* **2004**, *374*, 374.
12. Liang, J. Z.; Li, R. K. Y. *J. Appl. Polym. Sci.*, **2000**, *77*, 409.
13. Mae, H.; Omiya, M.; Kishimoto, K. *J. Appl. Polym. Sci.*, **2008**, *37*, 1561.
14. Wei, X. G.; Sue, J. H.; Chu, J.; Huang, C.; Gong, K. *J. Mater. Sci.* **1996**, *35*, 125.
15. Champagne, M. F.; Huneault, M. A.; Roux, C.; Peyrel, W. *Polym. Eng. Sci.* **1999**, *39*, 976.
16. Srinivasan, K. R.; Gupta, A. K. *J. Appl. Polym. Sci.* **1994**, *53*, 1.
17. Nakmaura, S.; Tokumitsu, K.; Kitamura, M.; Miyagawa, E.; Kanzawa, T.; Tanaka, A. *Resour. Process.* **2008**, *55*, 56.
18. Yazdani-Pedram, M.; Quijada, R.; López-Manchado, M. A. *Macromol. Mater. Eng.* **2003**, *288*, 875.
19. Duvall, J.; Sellitti, C.; Myers, C.; Hiltner, A.; Baer, E. *J. Appl. Polym. Sci.* **1994**, *52*, 195.
20. Holsti-miettinen, R.; Seppala, J. *Polym. Eng. Sci.* **1992**, *32*, 868.
21. Ide F.; Hasegawa, A. *J. Appl. Polym. Sci.* **1974**, *18*, 963.
22. Fouassier, J. P.; Rabek, J. F. *Radiation Curing in Polymer Science and Technology*, **1993**, 193.
23. Yoshii, F.; Sasaki, T.; Makuuchi, K.; Tamura, N. *JJMI* **1985**, *55*, 251.
24. Yoshii, F.; Sunaga, H.; Makuuchi, K.; Ishigaki, I.; Bahari, K. *JJMI* **1985**, *61*, 387.
25. Black, R. M.; Lyons, B. J. *Proc. R. Soc. Lond.* **1959**, *A253*, 322.
26. Mathakari, N. L.; Bhoraskar, V. N.; Dhole, S. D. *Nucl. Instrum. Methods Phys. Res.* **2008**, *266*, 3075.
27. Aymes-Chodur, C.; Betz, N.; Legendre, B.; Yagoubi, N. *Polym. Degrad. Stab.* **2006**, *91*, 649.
28. Charlesby, A. *Atomic Radiation and Polymers*; Pergamon Press: Oxford, **1960**; Vol. 123.
29. Sawasaki, T.; Nojiri, A. *Radiat. Phys. Chem.* **1988**, *31*, 877.
30. Han, D. H.; Shin, S. H.; Petrov, S. *Radiat. Phys. Chem.* **2004**, *69*, 239.
31. Steller, R.; Zuchowska, D.; Meissner, W.; Paukszta, D.; Garbarczyk, J. *Radiat. Phys. Chem.* **2006**, *75*, 259.
32. Van Gisbergen, J. G. M.; Meijer, H. E. H.; Lemstra, P. J. *Polymer* **1989**, *30*, 2153.
33. Aytac, A.; Deniz, V.; Sen, M.; Hegazy, E.; Guven, O. *Radiat. Phys. Chem.* **2010**, *79*, 297.
34. Pramanik, N. K.; Haldar, R.S.; Bhardwaj, Y. K.; Sabharwal, S.; Niyogi, U. K. Khandal, R. K. *J. Appl. Polym. Sci.*, **2011**, *122*, 193.
35. Ali, Z. I.; Said, H. M.; Youssef, H. A.; Saleh, H. H. *Polym. Plast. Technol. Eng.* **2005**, *44*, 1025.
36. Sethi, M.; Gupta, N. K.; Srivastava, A. K. *J. Appl. Polym. Sci.* **2002**, *86*, 2429.
37. Kumara, P. H. S.; Nagasawa, N.; Yagi, T.; Tamada, M. *J. Appl. Polym. Sci.* **2008**, *109*, 3321.
38. Branik, I.; Bhowmick, A. K. *Radiat. Phys. Chem.* **2000**, *58*, 293.
39. Drobny, J. G. *Radiation Technology for Polymers*; CRC Press LCC: Boca Raton, Florida, **2003**; Vol. 97.
40. Datta, S.; Singha, N. K.; Naskar, K.; Bhardwaj, Y. K.; Sabharwal, S. *J. Appl. Polym. Sci.* **2010**, *115*, 2573.
41. Bersted, B. H. *J. Appl. Polym. Sci.*, **1979**, *24*, 37.
42. Gonzalez, J.; Albano, C.; Ichazo, M.; Diaz, B. *Eur. Polym. J.* **2002**, *38*, 2465.